

Probability of Immobilization on Host Cell Surface Regulates Viral Infectivity

Michael C. DeSantis¹, Chunjuan Tian,¹ Jin H. Kim¹, Jamie L. Austin,¹ and Wei Cheng^{1,2,*}

¹Department of Pharmaceutical Sciences, University of Michigan, Ann Arbor, Michigan 48109, USA

²Department of Biological Chemistry, University of Michigan Medical School, Ann Arbor, Michigan 48109, USA



(Received 12 April 2020; accepted 18 August 2020; published 14 September 2020)

The efficiency of a virus to establish its infection in host cells varies broadly among viruses. It remains unclear if there is a key step in this process that controls viral infectivity. To address this question, we use single-particle tracking and Brownian dynamics simulation to examine human immunodeficiency virus type 1 (HIV-1) infection in cell culture. We find that the frequency of viral-cell encounters is consistent with diffusion-limited interactions. However, even under the most favorable conditions, only 1% of the viruses can become immobilized on cell surface and subsequently enter the cell. This is a result of weak interaction between viral surface gp120 and CD4 receptor, which is insufficient to form a stable complex the majority of the time. We provide the first direct quantitation for efficiencies of these events relevant to measured HIV-1 infectivity and demonstrate that immobilization on host cell surface post-virion-diffusion is the key step in viral infection. Variation of its probability controls the efficiency of a virus to infect its host cells. These results explain the low infectivity of cell-free HIV-1 *in vitro* and offer a potential rationale for the pervasive high efficiency of cell-to-cell transmission of animal viruses.

DOI: 10.1103/PhysRevLett.125.128101

Virions must go through many steps within their life cycle to establish infection in their host cells [1]. This process can be modeled as a Markov chain [2], with the occurrence of each step at a finite probability that is subject to thermal fluctuations [3]. Although a single virion can produce infection, the observed efficiency of infection actually differs widely among viruses of different families [1]. This efficiency of infection, i.e., infectivity, can be rigorously defined and measured as the percentage of initial total virions that establish productive infection in a cell-based assay *in vitro*. Bacteriophage T4 has an infectivity approaching 100%. However, this is not true for most animal viruses. Even under the most favorable culture conditions, the infectivity typically ranges from 0.1% to 10%. Although it is conceivable that different viruses have evolved different strategies for coping with their infection, an investigation of the underlined processes will be useful for quantitative understanding of this phenomenon.

We have used the human immunodeficiency virus type 1 (HIV-1), the causative agent of acquired immunodeficiency syndrome (AIDS), as our model system to understand the biophysical events in viral life cycle [4] that may limit viral infection. HIV-1 uses its surface glycoprotein gp120 for binding with CD4 and chemokine coreceptors to gain entry into host cells [5]. As we have studied previously, the infectivity of these virions varies between 0% and 1% [6–8] in cell culture. In order to gain a mechanistic understanding about this infectivity, here we have used the technique of single-particle tracking (SPT) [9–11] to image virion-cell interactions in real time, under the same conditions that we performed the infection assay.

To enable SPT with sufficient spatial and temporal resolution, we prepared HIV-1 virions carrying genetically encoded mCherry fluorophores confined to the interior space of the virion [12], following the protocols we established [6]. This labeling strategy ensures that individual virions possess sufficient numbers of fluorophores with high signal-to-noise ratio so that they can be tracked at short exposure times to achieve high spatio-temporal resolution. Meanwhile, the incorporation of fluorescent proteins into individual virions can be optimized so that the infectivity of fluorescently labeled virions is comparable to that of wild-type viruses [6]. To identify the potential bottleneck that may limit HIV-1 infectivity, we first examined the free diffusion of HIV-1 virions in culture media by high-speed imaging. Offline analysis of the corresponding fluorescence imaging videos permitted detection of individual virions in each frame, lateral positions of the virion, and a diffusion coefficient of $2.24 \pm 0.075 \mu\text{m}^2/\text{s}$ at 20 °C (Fig. S1, Supplemental Material [13]). The errors reported are standard errors of the mean (408 particles in this case) unless otherwise noted. This diffusion coefficient yields a mean diameter of 144 nm for a spherical particle, in good agreement with the average diameter of 145 nm as reported for single HIV-1 virions by cryoelectron microscopy studies [14]. Together, these results indicate that a single HIV-1 virion behaves as a normal Brownian particle in the culture media. It is therefore capable of engaging the target cell surface at a diffusion-limited rate.

We then used high-speed imaging to track single virions immediately upon incubation with TZM-bl cells, a standard

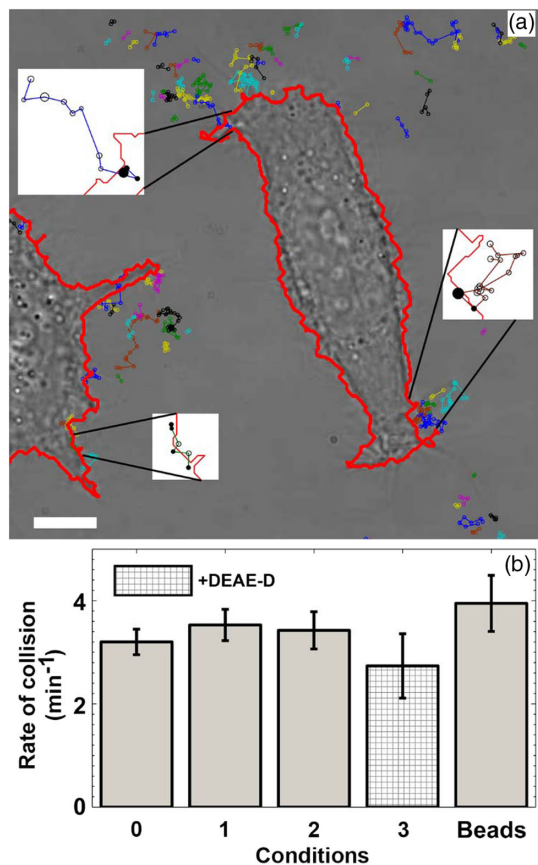


FIG. 1. Imaging and quantifying the dynamics of HIV-1 and TZM-bl interactions at short timescales. (a) High-speed imaging allows reconstruction of multiple tracks of HIV-1 virions from a 1000-frame video overlaid on a differential interference contrast image of the cells (boundaries outlined in red solid lines). The scale bar is $10\ \mu\text{m}$. (b) The rates of collision measured for HIV-1 virions under various conditions and for reference fluorescent beads with a mean diameter of $140\ \text{nm}$.

cell line for HIV-1 infection [15,16] that we have used [6–8]. These experiments were conducted at 37°C in chambered cover glass to closely mimic the conditions for measurement of virion infectivity [6]. Representative tracks identified for single virions in the presence of TZM-bl cells are shown in Fig. 1(a) as circles connected by solid lines in various colors (see also Video S1 in the Supplemental Material [13]). Each circle represents the centroid location of diffusing virions identified from the consecutive frames in high-speed videos, which are connected in sequence. The localization error from 2D-Gaussian fitting is reflected in the size of these circles, with a bigger size representing larger error, which are visible on three enlarged tracks above a white background (Fig. 1(a) insets). Throughout, the localization errors range from 13 to $140\ \text{nm}$, with an arithmetic mean of $39\ \text{nm}$. We have developed a method to discern viral-cell encounters that takes into account the localization errors for individual virions (Supplemental Material [13]). Using this method,

we have identified all the virion tracks within a video that had contact with a target cell surface at least once and calculated the rate of virion-cell encounter as the number of the initial encounters over the duration of each video. An average rate of collision was then plotted in Fig. 1(b) for the following HIV-1 virions used in this study: HIV_{0,0} without gp120 (condition 0), HIV_{0,2} with 4.5 ± 0.6 ($N = 119$) gp120 molecules per particle determined from optical trapping virometry experiments [7,8] (condition 1), HIV_{1,0} with 5.9 ± 0.7 ($N = 129$) gp120 molecules per particle (conditions 2 and 3), and also reference fluorescent polystyrene beads of $140\ \text{nm}$ diameter for comparison. The collision rates that we measured for various HIV-1 virions from these high-speed videos varied between 2.7 and $3.9\ \text{min}^{-1}$ [Fig. 1(b)]. The one-way analysis of variance (ANOVA) test conducted for these data yielded p values >0.05 for all five groups of data, demonstrating that these rates of collision are statistically indistinguishable from that of the reference polystyrene beads, independent of gp120 content per virion, and also independent of a polycation, diethylaminoethyl-dextran (DEAE-D) that was routinely used to enhance HIV-1 infectivity (condition 3). This result suggests that the initial encounter between a virion and its target cell is governed by Brownian diffusion instead of by gp120-specific or DEAE-D-mediated interactions. This is expected given the small debye length in water at physiological ionic strength ($<1\ \text{nm}$) [17]; electrostatic interactions will only become significant once the particle is very close to cell surface. The similarity of these rates to

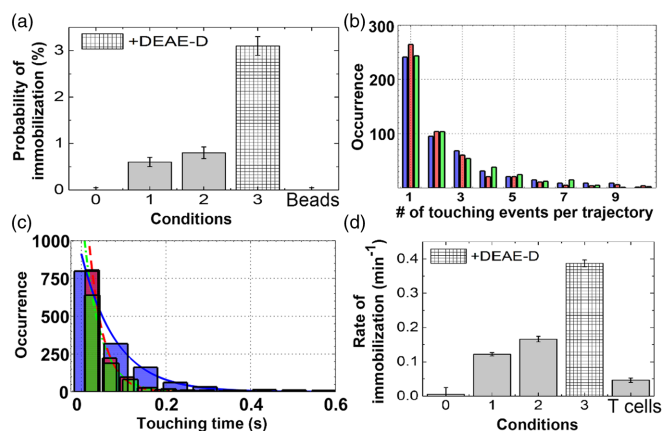


FIG. 2. Virion immobilization and the dynamics of transient virion-cell encounters. (a) Probability of immobilization determined for various particles and conditions. (b),(c) Histograms for number of touching events per trajectory and touching times determined for HIV_{0,0} (green), HIV_{0,2} (red), and HIV_{1,0} virions (blue) in the absence of DEAE-D. Histograms in (c) were fit by single-exponential functions for HIV_{0,0} (green dash-dotted line), HIV_{0,2} (red dashed line), and HIV_{1,0} virions (blue solid line). The number of tracks for each virion population in (b) and (c) were 409, 512, and 359, respectively. (d) Rate of immobilization determined for various conditions. In both (a) and (d), conditions 0, 1, 2, 3, and beads are for TZM-bl cells.

that of fluorescent polystyrene beads at the same particle concentrations further supports this notion, indicating that diffusion primarily governs the rate of initial viral-cell contact with little influence from particle compositions or the presence of DEAE-D.

To rationalize the above observations, we have done theoretical estimations for the rate of virion-cell collision using two different approaches. The first is based on the Smoluchowski equation [18] to estimate the association rate between a virion particle and a target cell. Using a diffusion coefficient of $3.16 \mu\text{m}^2/\text{s}$ for HIV-1 virions that we measured at 37°C , we estimate the association rate constant to be on the order of $\sim 10^{11} \text{M}^{-1} \text{s}^{-1}$. Our imaging experiments used a virion concentration of 1.13×10^8 particles/mL. This predicts a theoretical collision rate of 1.5min^{-1} under the current condition. This value is comparable in magnitude to our experimental measurement, suggesting that viral-cell encounters are indeed diffusion limited. The higher experimental values may be related to the fact that only videos containing virion-cell encounters were included in this analysis, which naturally bias the collision rates toward higher values. Our second theoretical approach is Brownian dynamics simulations (Fig. S2, Supplemental Material [13]), which is well suited for simulations of particle and cell encounters [19]. This set of simulations was done by releasing virion particles at varied distances from the target cell surface and measuring the return time and the percentage of virions that encountered the cell within a maximum allowance time of 4 min (Supplemental Material [13]). At a releasing distance of $14 \mu\text{m}$, which corresponded to the average distance between a virion and the cell surface at the viral concentration we used, the return time averaged from 5000 simulated particles is 40 s, which predicts a collision rate of 1.5min^{-1} and is also comparable in magnitude to our experimental measurements. These theoretical estimations support that diffusion indeed dominates the rate of virion-cell encounters under these experimental conditions.

Although we have experimentally identified a large number of virion tracks that contained at least one collision event with target cells, strikingly, greater than 97% of these virion tracks were “futile”; i.e., they ended up with a permanent dissociation instead of attachment or entry into the cells. This observation was true throughout the 2-h imaging window during which cells were incubated with virions, suggesting the existence of a bottleneck in gp120 and receptor interactions that limits HIV-1 infectivity. To identify this bottleneck, we conducted a set of quantitative analysis of individual virion tracks that encountered cells. First, to quantitate the percentage of virions that became immobilized in the end, i.e., attachment occurred, we defined the probability of immobilization as the ratio between the number of observed immobilization events and the total number of tracks comprising at least one collision event with the cell surface. This probability was

plotted in Fig. 2(a) for particles of various conditions, which showed a clear dependence on gp120 content per particle and also on the presence of DEAE-D in the culture media. We collected 198 videos for HIV_{0.0} without gp120 (condition 0), which yielded over 600 individual tracks. None of these tracks showed immobilization on the cell surface. The same was true for fluorescent polystyrene beads (182 videos). However, the probability of immobilization increased to 0.6% for HIV_{0.2} (condition 1) and to 0.8% for HIV_{1.0} (condition 2), respectively. These results demonstrate that, in the absence of DEAE-D, the attachment of HIV-1 virions is exclusively mediated by viral envelope glycoprotein gp120. For HIV_{1.0}, this probability further increased to 3.1% in the presence of DEAE-D (condition 3). This means that the probability of immobilization can be enhanced in the presence DEAE-D, which is well correlated with the effect of DEAE-D in enhancing virion infectivity.

What happened to those futile diffusing virions? Although these HIV-1 virions escaped from the cell surface eventually, many of their tracks exhibited multiple transient contacts with the cell surface before their final dissociation, as revealed by our high-speed imaging [inserts to Fig. 1(a)]. Detailed statistics of this phenomenon are shown in Fig. 2(b), which plots the histograms for the number of touching events per trajectory from HIV_{0.0} (green), HIV_{0.2} (red), and HIV_{1.0} (blue), in the absence of DEAE-D. These histograms showed that over half of all tracks displayed at least two transient contacts with target cells, regardless of gp120 content per virion. This repeated “kiss-and-run” phenomenon [9] is consistent with the diffusion of a Brownian particle near a solid surface, where the particle typically undergoes multiple microscopic collisions with the surface before its permanent dissociation. However, the touching time [9], i.e., the time that a virion spent in each transient but continuous contact with the cell membrane, displayed a different trend, as shown in Fig. 2(c) for the histograms we constructed for HIV_{0.0} (green), HIV_{0.2} (red), and HIV_{1.0} (blue), in the absence of DEAE-D. These histograms were best fit with single-exponential functions, which yielded a relaxation time constant of 39.7 ± 0.05 , 34.1 ± 0.04 , and 82.1 ± 0.06 ms for HIV_{0.0}, HIV_{0.2}, and HIV_{1.0}, respectively. The one-way ANOVA test conducted for these data revealed that we cannot tell the difference between HIV_{0.0} and HIV_{0.2}, likely because these values were close to our camera exposure time of 10 ms. However, the distribution of touching times for HIV_{1.0} is statistically different from the other two distributions (p value = 0.002). This analysis indicates that gp120-specific interactions were actually formed during these transient touches between virions and cells. However, these transient contacts were not strong enough to hold onto the virion particle, and additional viral-cell interactions are required for immobilization. Figure 2(d) shows the rates of virion immobilization that we have measured under various

conditions, defined as the number of immobilized virions over the total duration of all videos collected. Compared to Fig. 1(b), the rates of immobilization for various virions overall were slower than the rates of virion-cell collision by more than tenfold. This is a direct consequence of the low probability of virion immobilization on cell surface, even though these virions can approach cell surface at diffusion-limited rates. TZM-bl is an engineered HeLa cell line that has been selected to be highly susceptible to infection by diverse isolates of HIV-1 [20]. This cell line expresses $\sim 4 \times 10^5$ CD4 molecules per cell [20,21], which is much higher than CD4⁺ T cells [22]. For comparison, we also imaged the interactions between HIV_{1.0} and SUP-T1 cells, which was a nonengineered T cell line that expressed CD4 [23]. As shown in the last column of Fig. 2(d), the rate of virion immobilization was in fact lower than that on TZM-bl cells, consistent with a lower CD4 receptor density on SUP-T1 cell surface.

The above results reveal that attachment of a HIV-1 virion on target cell surface in cell culture *in vitro* is limited by a rather inefficient immobilization step post-virion-diffusion. A single trip of a virion, which may include multiple collisions with the cell surface, is usually not sufficient to establish a stable attachment of an HIV-1 virion on the cell surface, despite the fact that target cells have a high surface expression of CD4 receptors and that gp120-specific interactions have taken place. This result is consistent with the literature that trimeric gp120 on virion surface has low affinity toward CD4 [24], and gp120 trimer on native intact virions stays most of the time in a closed conformation that only occasionally samples the conformation that is conducive to CD4 receptor binding [25]. On the other hand, multiple gp120 and receptor pair interactions have been implicated in HIV entry and productive infection [7,26,27], which, in principle, can promote stronger binding through multiple weak interactions and therefore immobilization on cell surface. The slight increase in the rate of immobilization with increasing gp120 content per virion is consistent with this notion [Fig. 2(d), conditions 1 and 2, p value = 0.003 from a two-sample T test].

To confirm the relevance of the above measurements to HIV-1 infection, it is necessary to examine the fate of those immobilized virions. We used time-lapse imaging at a frame rate of 1 Hz to minimize photobleaching and continuously recorded virion tracks over the 2-h incubation period. Representative tracks of single virions from time-lapse imaging are shown in Fig. 3(a) (Video S2, Supplemental Material [13]). A substantial portion of immobilized virions were internalized into target cells, as indicated by their highly restricted motions inside the cytosol. These tracks are labeled as 1–8 in Fig. 3(a), which are in sharp contrast to freely diffusing virions [unlabeled tracks in Fig. 3(a)] in the scales of motion. The efficiency of this internalization, i.e., the number of internalized virions

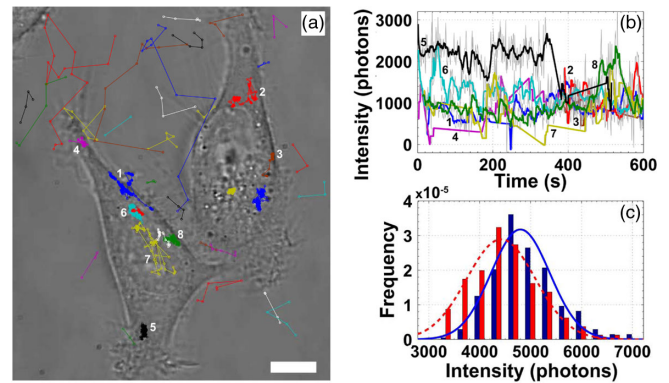


FIG. 3. Time-lapse imaging of HIV_{1.0} and TZM-bl interactions and the dynamics of internalized virions. (a) While many virions transiently interact at the cell surface before diffusing away, virion immobilization and internalization can be clearly identified (tracks 1–8). In particular, track 7 can undergo extensive intracellular transport. The scale bar is 10 μm . (b) Corresponding boxcar-filtered fluorescence intensities using a 10-s wide window for the labeled tracks in (a). (c) Distributions of measured intensities for freely diffusing (blue bars) and internalized HIV_{1.0} virions (red bars) at focus.

over all immobilized virions, is 71.2% ($N = 98$) for HIV_{0.2} and 74.3% ($N = 102$) for HIV_{1.0}, respectively, in the absence of DEAE-D in TZM-bl cells. This means that once immobilized on cell surface, most virions could further proceed to enter cells with high efficiencies. For the majority of these internalization events, the fluorescence intensities from individual virions were long-lived, as shown in the time courses in Fig. 3(b), taken from tracks 1–8 in Fig. 3(a). The apparent jumps in these intensity time traces were due to virion diffusion to or away from the imaging plane. To assess the level of photobleaching, we constructed a histogram of the fluorescence intensities for these virions corresponding to the last frame they were at focus [Fig. 3(c), red bars] and compared it to that of the intensities of freely diffusing virions in culture media [Fig. 3(c), blue bars]. Both histograms were well described by Gaussian distributions (solid and dashed lines), with means that differed by $\sim 10\%$, suggesting a minimal effect of photobleaching. This result also suggests that, during this time window of analysis, virion cores remain intact, consistent with endocytosis as the route for productive infection in TZM-bl cell line [28].

In summary, we have quantitated the series of kinetic events during early steps of HIV-1 infection in cell culture, i.e., diffusion, immobilization, and internalization. In conjunction with infectivity measured under the same conditions, these results reveal that virion immobilization, an intermediate step between diffusion and internalization, is a unique point of regulation for viral infectivity. Because the rest of the intracellular steps occurs with a much higher efficiency, slight variation in the probability of virion immobilization can substantially

influence the resulting viral infectivity (Fig. S3, Supplemental Material [13]). For the first time, we directly visualized that gp120-specific interaction can form upon virion-cell collision, but in many cases this initial interaction is too weak to immobilize the virus. These results uncover an unexpected similarity to bacteriophage T4, a highly sophisticated DNA-injection nanomachinery. Despite being a remote virus from HIV-1 in their evolution, the immobilization of T4 virus on bacterial surface requires a minimum of three long tail fibers that have bound to cell surface receptors, otherwise the virus remains mobile [29]. Our conclusions may also be relevant for molecular understanding of coronavirus disease 2019 pandemic caused by severe acute respiratory syndrome coronavirus 2, which has a spike protein with high affinity toward its receptor angiotensin converting enzyme 2 (ACE2) [30], and children have a lower expression of ACE2 in nasal epithelium than adults [31]. Different probability of immobilization may give rise to varying degrees of infectivity, which can be tested experimentally.

The low efficiency of HIV-1 immobilization revealed from the current study is limited by its *in vitro* settings and no definitive conclusions can be drawn for situations *in vivo*. However, because immobilization on host cell surface is an obligate step for cell-free virions to establish their infection regardless of the complexity of environments, our results also have implications on HIV-1 infection *in vivo*. The survival of virions is finite as determined by both their intrinsic stability [32] and cellular mechanisms that can inactivate virions [33]. We therefore expect that any mechanism that can alter the efficiency of virion immobilization on host cell surface will have a direct impact on HIV-1 infectivity both *in vitro* and likely *in vivo*. For example, semen-derived amyloid fibers can promote HIV-1 immobilization on target cells and enhance viral infectivity by several orders of magnitude [34]. The excluded volume effect as a result of the narrow and confined intercellular space in both virological synapse and gut-associated lymphoid tissues [35,36] [Fig. S4(a), Supplemental Material [13]] can greatly decrease the time for virion diffusion and enhance the rate of virion-cell encounter, as indicated by our Brownian dynamics simulations (Fig. S2), and lead to increased infectivity [37,38]. The current study provides the quantitative information needed for people to model the early events of HIV-1 infection in various biological contexts [Fig. S4(b) in the Supplemental Material [13], which includes Refs. [39–58]].

We acknowledge NIH/NIAID Grant No. 1R21AI135559-01A1 to W.C., MCubed Project No. 8290 and the Team Science Award to W.C. by the University of Michigan, NIH Director's New Innovator Award No. 1DP2OD008693-01 to W.C., and also a Research Grant No. 5-FY10-490 to W.C. from the

March of Dimes Foundation. M. C. D. was supported by a NIH postdoctoral fellowship awarded under F32-GM109771. We thank Alice Telesnitsky for helpful discussions. We thank Benjamin K. Chen for HIV-iGFP plasmids. The following reagents were obtained through the AIDS Research and Reference Reagent Program, Division of AIDS, National Institute of Allergy and Infectious Diseases (NIAID), National Institutes of Health (NIH): pNL4-3 from Dr. Malcolm Martin; pNL4-3.Luc.R-E- from Dr. Nathaniel Landau; TZM-bl cells from Dr. John C. Kappes, Dr. Xiaoyun Wu, and Tranzyme, Inc.; and SUP-T1 cells from Dr. James Hoxie.

Author contributions: W. C. conceived and directed the project; M. C. D., C. T., J. H. K., and J. L. A. prepared experimental materials; M. C. D. and W. C. conducted the experiments; M. C. D. and W. C. performed the analysis; M. C. D. and W. C. wrote the paper.

*Corresponding author.
chengwe@umich.edu

- [1] D. M. Knipe and P. M. Howley, *Fields Virology*, 6th ed. (Wolters Kluwer/Lippincott Williams & Wilkins Health, Philadelphia, PA, 2013).
- [2] F. S. Heldt, S. Y. Kupke, S. Dorl, U. Reichl, and T. Frensing, *Nat. Commun.* **6**, 8938 (2015).
- [3] A. C. Barato and U. Seifert, *Phys. Rev. Lett.* **114**, 158101 (2015).
- [4] D. D. Ho and P. D. Bieniasz, *Cell* **133**, 561 (2008).
- [5] R. Wyatt and J. Sodroski, *Science* **280**, 1884 (1998).
- [6] J. H. Kim, H. Song, J. L. Austin, and W. Cheng, *PLoS One* **8**, e67170 (2013).
- [7] M. C. DeSantis, J. H. Kim, H. Song, P. J. Klasse, and W. Cheng, *J. Biol. Chem.* **291**, 13088 (2016).
- [8] Y. Pang, H. Song, J. H. Kim, X. Hou, and W. Cheng, *Nat. Nanotechnol.* **9**, 624 (2014).
- [9] G. Seisenberger, M. U. Ried, T. Endress, H. Buning, M. Hallek, and C. Brauchle, *Science* **294**, 1929 (2001).
- [10] E. Rothenberg, L. A. Sepulveda, S. O. Skinner, L. Zeng, P. R. Selvin, and I. Golding, *Biophys. J.* **100**, 2875 (2011).
- [11] K. Welsher and H. Yang, *Nat. Nanotechnol.* **9**, 198 (2014).
- [12] W. Hubner, P. Chen, A. Del Portillo, Y. Liu, R. E. Gordon, and B. K. Chen, *J. Virol.* **81**, 12596 (2007).
- [13] See Supplemental Material at <http://link.aps.org/supplemental/10.1103/PhysRevLett.125.128101> for materials and methods, supplemental figures and videos.
- [14] J. A. G. Briggs, T. Wilk, R. Welker, H. G. Krausslich, and S. D. Fuller, *EMBO J.* **22**, 1707 (2003).
- [15] C. A. Derdeyn, J. M. Decker, J. N. Sfakianos, X. Wu, W. A. O'Brien, L. Ratner, J. C. Kappes, G. M. Shaw, and E. Hunter, *J. Virol.* **74**, 8358 (2000).
- [16] X. Wei *et al.*, *Antimicrob. Agents Chemother.* **46**, 1896 (2002).
- [17] O. Malysheva, T. Tang, and P. Schiavone, *J. Colloid Interface Sci.* **327**, 251 (2008).

- [18] R. M. Noyes, *Prog. React. Kinet. Mech.* **1**, 129 (1961).
- [19] T. J. English and D. A. Hammer, *Biophys. J.* **86**, 3359 (2004).
- [20] E. J. Platt, M. Bilaska, S. L. Kozak, D. Kabat, and D. C. Montefiori, *J. Virol.* **83**, 8289 (2009).
- [21] E. J. Platt, K. Wehrly, S. E. Kuhmann, B. Chesebro, and D. Kabat, *J. Virol.* **72**, 2855 (1998).
- [22] M. A. Nokta, X. D. Li, J. Nichols, M. Mallen, A. Pou, D. Asmuth, and R. B. Pollard, *AIDS* **15**, 161 (2001).
- [23] S. D. Smith, M. Shatsky, P. S. Cohen, R. Warnke, M. P. Link, and B. E. Glader, *Cancer Res.* **44**, 5657 (1984), <https://pubmed.ncbi.nlm.nih.gov/6437672/>.
- [24] S. Ugolini, I. Mondor, and Q. J. Sattentau, *Trends Microbiol.* **7**, 144 (1999).
- [25] J. B. Munro *et al.*, *Science* **346**, 759 (2014).
- [26] R. Sougrat, A. Bartesaghi, J. D. Lifson, A. E. Bennett, J. W. Bess, D. J. Zabransky, and S. Subramaniam, *PLoS Pathogens* **3**, e63 (2007).
- [27] J. Chojnacki, T. Staudt, B. Glass, P. Bingen, J. Engelhardt, M. Anders, J. Schneider, B. Muller, S. W. Hell, and H.-G. Krausslich, *Science* **338**, 524 (2012).
- [28] K. Miyauchi, Y. Kim, O. Latinovic, V. Morozov, and G. B. Melikyan, *Cell* **137**, 433 (2009).
- [29] M. G. Rossmann, V. V. Mesyanzhinov, F. Arisaka, and P. G. Leiman, *Curr. Opin. Struct. Biol.* **14**, 171 (2004).
- [30] D. Wrapp, N. Wang, K. S. Corbett, J. A. Goldsmith, C. L. Hsieh, O. Abiona, B. S. Graham, and J. S. McLellan, *Science* **367**, 1260 (2020).
- [31] S. Bunyavanich, A. Do, and A. Vicencio, *JAMA* **323**, 2427 (2020).
- [32] S. P. Layne, M. J. Merges, M. Dembo, J. L. Spouge, S. R. Conley, J. P. Moore, J. L. Raina, H. Renz, H. R. Gelderblom, and P. L. Narat, *Virology* **189**, 695 (1992).
- [33] Y. Choi, J. W. Bowman, and J. U. Jung, *Nat. Rev. Microbiol.* **16**, 341 (2018).
- [34] J. Munch *et al.*, *Cell* **131**, 1059 (2007).
- [35] N. Martin, S. Welsch, C. Jolly, J. A. G. Briggs, D. Vaux, and Q. J. Sattentau, *J. Virol.* **84**, 3516 (2010).
- [36] M. S. Ladinsky, C. Kieffer, G. Olson, M. Deruaz, V. Vrbancac, A. M. Tager, D. S. Kwon, and P. J. Bjorkman, *PLoS Pathogens* **10**, e1003899 (2014).
- [37] Q. Sattentau, *Nat. Rev. Microbiol.* **6**, 815 (2008).
- [38] P. Zhong, L. M. Agosto, J. B. Munro, and W. Mothes, *Curr. Opin. Virol.* **3**, 44 (2013).
- [39] J. C. Olivo-Marin, *Pattern Recognit.* **35**, 1989 (2002).
- [40] M. C. DeSantis, S. H. DeCenzo, J. L. Li, and Y. M. Wang, *Opt. Express* **18**, 6563 (2010).
- [41] R. E. Thompson, D. R. Larson, and W. W. Webb, *Biophys. J.* **82**, 2775 (2002).
- [42] J. C. Crocker and D. G. Grier, *J. Colloid Interface Sci.* **179**, 298 (1996).
- [43] H. Qian, M. P. Sheetz, and E. L. Elson, *Biophys. J.* **60**, 910 (1991).
- [44] Y. M. Wang, R. H. Austin, and E. C. Cox, *Phys. Rev. Lett.* **97**, 048302 (2006).
- [45] F. C. Collins, *J. Colloid Sci.* **5**, 499 (1950).
- [46] M. C. DeSantis, J. L. Li, and Y. M. Wang, *Phys. Rev. E* **83**, 021907 (2011).
- [47] H. Brenner, *Chem. Eng. Sci.* **16**, 242 (1961).
- [48] H. C. Berg, *Random Walks in Biology*, expanded edition (Princeton University Press, Princeton, NJ, 1993).
- [49] J. A. Thomas, D. E. Ott, and R. J. Gorelick, *J. Virol.* **81**, 4367 (2007).
- [50] O. G. Berg and P. H. von Hippel, *Annu. Rev. Biophys. Biophys. Chem.* **14**, 131 (1985).
- [51] A. T. Haase, *Nature (London)* **464**, 217 (2010).
- [52] A. M. Carias *et al.*, *J. Virol.* **87**, 11388 (2013).
- [53] A. M. Carias and T. J. Hope, *Curr. Immunol. Rev.* **15**, 4 (2019).
- [54] Z. Zhang *et al.*, *Science* **286**, 1353 (1999).
- [55] D. J. Anderson, J. Marathe, and J. Pudney, *Am. J. Reprod. Immunol.* **71**, 618 (2014).
- [56] A. T. Haase, *Nat. Rev. Immunol.* **5**, 783 (2005).
- [57] N. F. Parrish *et al.*, *Proc. Natl. Acad. Sci. U.S.A.* **110**, 6626 (2013).
- [58] M. A. Swartz and M. E. Fleury, *Annu. Rev. Biomed. Eng.* **9**, 229 (2007).